

Subtraction and Addition of Propagating Photons by Two-Level Emitters

Mads M. Lund^{1,*}, Fan Yang^{2,*†}, Victor Rueskov Christiansen¹, Danil Kornovan¹, and Klaus Mølmer²

¹Center for Complex Quantum Systems, Department of Physics and Astronomy, Aarhus University, DK-8000 Aarhus C, Denmark

²Niels Bohr Institute, University of Copenhagen, Blegdamsvej 17, 2100 Copenhagen, Denmark

 (Received 24 April 2024; accepted 29 July 2024; published 4 September 2024)

Coherent manipulation of quantum states of light is key to photonic quantum information processing. In this Letter, we show that a passive two-level nonlinearity suffices to implement non-Gaussian quantum operations on propagating field modes. In particular, the collective light-matter interaction can efficiently extract a single photon from a multiphoton input wave packet to an orthogonal temporal mode. We accurately describe the single-photon subtraction process by elements of an intuitive quantum-trajectory model. By employing this process, quantum information protocols gain orders of magnitude improved efficiency over heralded schemes with linear optics. The reverse process can be used to add photons one by one to a single wave packet mode and compose arbitrarily large Fock states with a finite total success probability $>96.7\%$.

DOI: [10.1103/PhysRevLett.133.103601](https://doi.org/10.1103/PhysRevLett.133.103601)

Introduction—Propagating photons are ideal carriers of quantum information, since they can be precisely manipulated, detected, and distributed in a scalable manner [1–4]. While Gaussian operations such as beam splitting [5] and squeezing [6] are well established, efficient non-Gaussian operations are still under active development, as they are essential to exhaust the potential of bosonic fields in quantum computing and simulation [7–11].

Single-photon subtraction and addition are such non-Gaussian processes that have received considerable attention [12–16]. Based on beam splitters, squeezed light sources, and photon detection, heralded schemes exist for this purpose [17–21], but they succeed only with low probabilities. A number of nonlinear optical setups have been proposed to achieve more favorable deterministic operation, including so-called active schemes where an input pulse may be converted to a single cavity mode, affected by a subsequent unitary cavity QED interaction [22–24]. Passive schemes [25–30], in contrast may operate on the input pulse in a more robust, autonomous manner. However, the interaction of input photons with the nonlinear medium over time usually populates multiple field modes and results in a reduced purity of the states generated [31,32], which severely limits their practical applications in quantum information processing.

The saturation-type nonlinearity of a two-level emitter (TLE) coupled to a unidirectional continuum field [33–35] is conjectured to support single-photon subtractions, based on the intuitive argument, that the emitter can only absorb a

single photon at a time. In this Letter, we demonstrate that a passive two-level nonlinearity is, indeed, sufficient for single-photon subtraction. While all photons taking part in the dynamics could potentially scatter into a vast number of modes, we show that, provided the optimal duration of the input pulse, a single photon is converted to a temporal mode orthogonal to the original mode still occupied by the remaining photons [Fig. 1(a)]. This makes the conjugate process, adding a single photon to a Fock-state pulse by the same component [dashed arrows in Fig. 1(a)], equally efficient.

Single-photon subtraction—We consider the scattering of a unidirectional continuous field $\hat{\mathcal{E}}(t)$ by a TLE, as can be visualized by the chiral waveguide QED configuration shown in Fig. 1(a). The incoming field is in an n -photon Fock state $|n\rangle = (\hat{a}^\dagger)^n|0\rangle/\sqrt{n!}$, where $\hat{a}^\dagger = \int dt \phi_a(t)\hat{\mathcal{E}}^\dagger(t)$ creates a single photon in a given temporal mode $\phi_a(t)$. To investigate the scattering dynamics of

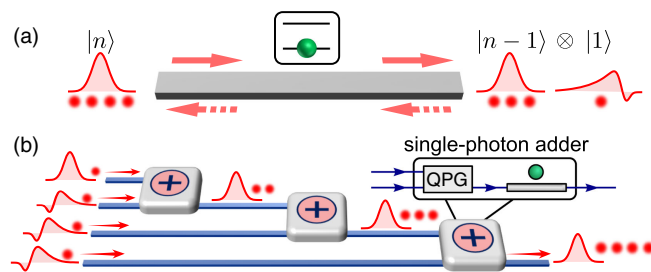


FIG. 1. (a) Schematic of the single-photon subtraction and addition mediated by a TLE. (b) Construction of a high photon number state from individual photons. The single-photon adder is composed of a QPG and a TLE.

*These authors contributed equally to this work.

†Contact author: fanyangphys@gmail.com

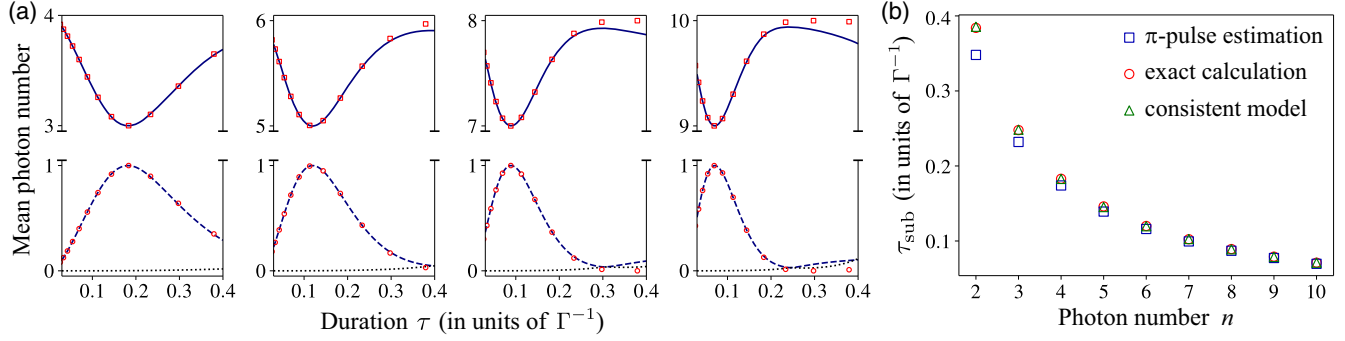


FIG. 2. Scattering of a single-mode input pulse by a TLE. (a) Mean photon number in different output modes as a function of the duration τ of the input Gaussian pulse. The four panels (from left to right) show the results for input photon number $n = 4, 6, 8,$ and 10 , respectively. The black solid line, the black dashed line, and the black dotted line show the mean photon number in the dominant mode (\bar{n}_1), the second dominant mode (\bar{n}_2), and the residual modes ($\sum_{i>2} \bar{n}_i$), respectively. The red squares and circles are obtained from a consistent model, presented in the text. (b) Duration τ_{sub} for achieving the optimal single-photon subtraction. The blue squares correspond to a simple π -pulse assumption. The red circles are obtained from the exact calculation of $\rho_{n-1, n-1}^a$. The green triangles are obtained from our consistent model.

such an input field pulse, we employ an adaption of the input-output formalism [36–38], which allows calculation of the correlations in the output field $\hat{\mathcal{E}}_{\text{out}}(t)$. In general, the output photons will not be restricted to the input mode but form a complicated time-frequency entangled state. To analyze the multimode character of the corresponding state, we carry out the Karhunen-Loève expansion of the first order correlation function, $\langle \hat{\mathcal{E}}_{\text{out}}^\dagger(t) \hat{\mathcal{E}}_{\text{out}}(t') \rangle = \sum_i \bar{n}_i \phi_i^*(t) \phi_i(t')$, where $\phi_i(t)$ denotes a set of orthonormal temporal modes and \bar{n}_i denotes the mean photon number in each mode [39].

Figure 2(a) shows the results of this expansion for different input Fock states $n = 4, 6, 8, 10$, where the mean photon number in the most populated mode (upper solid lines), the second most populated mode (middle dashed lines), and the rest of the modes (lower dotted lines) is plotted as a function of the duration τ of the input Gaussian pulse $\phi_a(t) \propto e^{-(t-4\tau)^2/2\tau^2}$. Evidently, for pulse durations shorter than the lifetime (Γ^{-1}) of the TLE, the first two modes ($i = 1, 2$) dominate the photon population in the output field with $\bar{n}_1 + \bar{n}_2 \approx n$. More interestingly, \bar{n}_1 and \bar{n}_2 attain values $\bar{n}_1 \approx n - 1$ and $\bar{n}_2 \approx 1$ at specific durations τ_{sub} , where the mode function $\phi_1(t)$ also approaches the input mode $\phi_a(t)$. Such a photon-number splitting is indicative of a perfect single-photon subtraction from the input field. To confirm that a single quantum has been removed, we examine the reduced density matrix $\hat{\rho}^a$ for output photons residing in the input mode $\phi_a(t)$ [36–38]. We find that the element $\rho_{n-1, n-1}^a = \langle n-1 | \hat{\rho}^a | n-1 \rangle$ indeed approaches unity (>0.996) at the optimal duration τ_{sub} , suggesting a successful subtraction of one photon from the input Fock state. Here, the subtracted photon is converted into a temporal mode $\phi_b(t) = \phi_2(t)$ orthogonal to the input mode $\phi_a(t)$. The output state is thus given by $|n-1\rangle \otimes |1\rangle = (\hat{a}^\dagger)^{n-1} \hat{b}^\dagger |0\rangle / \sqrt{(n-1)!}$, where $\hat{b}^\dagger = \int dt \phi_b(t) \hat{\mathcal{E}}^\dagger(t)$ creates a single photon in $\phi_b(t)$.

To understand why the TLE can behave as a perfect single-photon subtractor and how the optimal duration scales with the input photon number, we first consider a simplistic, intuitive model. By simply replacing the continuum with a single mode $\hat{\mathcal{E}}(t) \approx \phi_a(t) \hat{a}$, the light-matter interaction is described by a Jaynes-Cummings (JC) Hamiltonian $\hat{H} = i\sqrt{\Gamma} \phi_a(t) (\hat{a}^\dagger \hat{\sigma}_- - \hat{\sigma}_+ \hat{a})$, where $\hat{\sigma}_\pm$ denotes the spin raising and lowering operator of the TLE. Assuming an independent spontaneous emission process, the scattering can be depicted by the level diagram shown in Fig. 3(a), where the straight and the wavy arrows represent the coherent and the incoherent part of the dynamics, respectively. The interaction between the input field and the TLE first converts a photon from the single pulse mode oscillator into an atomic excitation $|n, g\rangle \rightarrow |n-1, e\rangle$. Then the spontaneous emission removes the

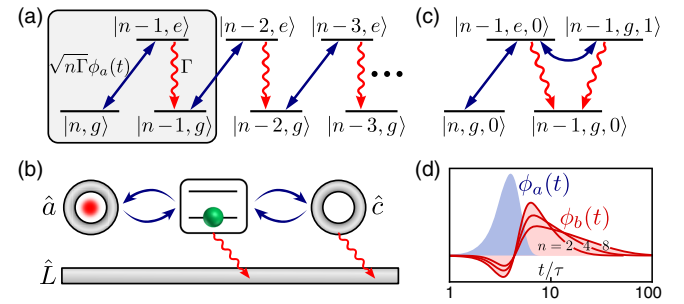


FIG. 3. (a) Level scheme for the intuitive JC model, where the shaded block indicates the truncated subspace populated by a short input pulse. (b) and (c) illustrate our consistent model incorporating an auxiliary mode and its (truncated) level scheme, respectively. (d) Shape of the input and output mode $\phi_a(t)$ and the singly occupied output mode $\phi_b(t)$ for the input photon number $n = 2, 4, 8$. The linewidth Γ is chosen to achieve the optimal subtraction for each n , and the horizontal axis is plotted in logarithmic scale.

TLE excitation from the system and leads to $|n-1, g\rangle$, which may be subsequently re-excited to $|n-2, e\rangle$ by the tail of the input field. For a short duration $\tau \lesssim \Gamma^{-1}$, the input pulse traverses the TLE before the completion of the spontaneous emission, such that only the first sector of the ladder [shaded block in Fig. 3(a)] is relevant. In this simplified picture, single-photon subtraction will therefore occur if the quantum Rabi oscillation dynamics executes a π -pulse [$2 \int dt \sqrt{n\Gamma} \phi_a(t) = \pi$] that perfectly transfers the initial state into $|n-1, e\rangle$. For Gaussian input modes, this yields an optimal duration $\tau_\pi = \pi^{3/2}/(8\Gamma n)$.

While this intuitive model provides a qualitative account of the observed photon subtraction, as shown in Fig. 2(b), it fails to reproduce the precise optimal duration τ_{sub} for small and intermediate photon numbers. More crucially, the model does not account properly for the spatiotemporal behavior of the subtracted photon and ensure that it is orthogonal to the input mode. These omissions stem from the single-mode approximation in the simplistic JC model, as the propagating light field is inherently multimode.

We develop here a consistent theory which can yield quantitative predictions while preserving the intuition offered by the JC model. To properly account for the interaction of the TLE with the multimode continuous field, we employ a recently developed approach [38], which corroborates the validity of the intuitive single-mode JC model, giving rise, however, to the additional coupling to an auxiliary single mode \hat{c} . In the interaction picture, the system dynamics is described by a Lindblad master equation with a Hamiltonian,

$$\hat{H} = i\sqrt{\Gamma}\phi_a^*(t)[\hat{a}^\dagger\hat{\sigma}_- + \cot 2\theta(t)\hat{c}^\dagger\hat{\sigma}_-] + \text{H.c.}, \quad (1)$$

and a single Lindblad dissipation term,

$$\hat{L} = \sqrt{\Gamma}\hat{\sigma}_- - 2\phi_a(t) \csc 2\theta(t)\hat{c}, \quad (2)$$

where $\theta(t)$ is defined as $\sin^2\theta(t) = \int_0^t d\xi |\phi_a(\xi)|^2$. The role of the auxiliary mode is illustrated in Fig. 3(b): it interacts coherently with the TLE, and its leakage interferes with the spontaneous emission from the emitter via the collective decay \hat{L} . This interference accurately describes the photon loss from the input mode, i.e., the subtracted photon and its wave function. Inclusion of the auxiliary mode results in a more complicated ladder of quantum states, but similar to Fig. 3(a), a truncation can be made for short input pulses. The truncated subspace is displayed in Fig. 3(c), where the initial state $|n, g, 0\rangle$ with the auxiliary mode in the vacuum state evolves via intermediate states $|n-1, e, 0\rangle$ and $|n-1, g, 1\rangle$ toward the photon-subtracted target state $|n-1, g, 0\rangle$.

We can now apply an efficient quantum-trajectory description of the dynamics [40–43], where the state follows a nonunitary evolution until the probabilistic

occurrence of a quantum jump by \hat{L} which removes an excitation from the system. As the truncated subspace allows only a single jump, the unnormalized wave function for the bath excitation (subtracted photon) is determined by

$$\tilde{\phi}_b(t) = \langle n-1, g, 0 | \hat{L} \cdot \hat{U}_{\text{eff}}(t, 0) | n, g, 0 \rangle. \quad (3)$$

Here, the nonunitary evolution operator $\hat{U}_{\text{eff}}(t, 0)$ is governed by $i\partial_t \hat{U}_{\text{eff}}(t, 0) = \hat{H}_{\text{eff}}(t) \hat{U}_{\text{eff}}(t, 0)$, with the non-Hermitian Hamiltonian $\hat{H}_{\text{eff}} = \hat{H} - i\hat{L}^\dagger \hat{L}/2$:

$$\hat{H}_{\text{eff}} = i \begin{bmatrix} 0 & \sqrt{n\Gamma}\phi_a^*(t) & 0 \\ -\sqrt{n\Gamma}\phi_a(t) & -\Gamma/2 & \sqrt{\Gamma}\phi_a(t)\tan\theta \\ 0 & \sqrt{\Gamma}\phi_a^*(t)\cot\theta & -2|\phi_a(t)\csc 2\theta|^2 \end{bmatrix}.$$

The evolved no-jump state $|\psi(t)\rangle = \hat{U}_{\text{eff}}(t, 0)|n, g, 0\rangle = |\psi(t)\rangle = C_1(t)|n, g, 0\rangle + C_2(t)|n-1, e, 0\rangle + C_3(t)|n-1, g, 1\rangle$ ultimately attains $C_1(\infty)|n, g, 0\rangle$, from which we can construct the output state of the photonic field,

$$|\Psi_{\text{out}}\rangle = C_1(\infty) \frac{(\hat{a}^\dagger)^n}{\sqrt{n!}} |0\rangle + \sqrt{P} \frac{(\hat{a}^\dagger)^{n-1}}{\sqrt{(n-1)!}} \hat{b}^\dagger |0\rangle, \quad (4)$$

where \hat{b}^\dagger creates a photon in the new temporal mode fed by the dissipation term \hat{L} (not to be confused with the C_3 auxiliary photon component), and $P = 1 - |C_1(\infty)|^2 = \int dt |\tilde{\phi}_b(t)|^2$ is the subtraction efficiency with $\tilde{\phi}_b(t) = \sqrt{\Gamma}C_2(t) - 2\phi_a(t) \csc 2\theta(t)C_3(t)$ obtained from Eq. (3). Compensating for the dispersion caused by the auxiliary mode [44], the normalized wave function for mode \hat{b} reads as

$$\phi_b(t) = \frac{1}{\sqrt{P}} \left[\tilde{\phi}_b(t) - \phi_a(t) \int_t^\infty d\xi \phi_a^*(\xi) \tilde{\phi}_b(\xi) \csc^2\theta(\xi) \right].$$

As illustrated in Fig. 3(d), while $\phi_b(t)$ has an exponential tail $\sim e^{-\Gamma t/2}$ being fed by the TLE spontaneous emission, its shape at earlier times is significantly modified and secures the orthogonality condition $\int dt \phi_a^*(t) \phi_b(t) = 0$.

The quantitative performance of our consistent theory is tested in Fig. 2(a), where we use Eq. (4) to obtain the output field correlation function and determine the two eigenmodes. The results (indicated by the squares and circles) agree well with the exact mode decomposition, while a visible deviation only appears at a large duration τ . In this region, the state $|n-1, g, 0\rangle$ accumulates non-negligible populations while the TLE still interacts with the input mode, which drives the system out of the truncated subspace in Fig. 3(c), and causes multiphoton and multimode subtracted components. We are interested in the single-photon subtraction regime where our consistent model can predict with high precision the optimal duration τ_{sub} of the

input mode [Fig. 2(c)] as well as the shape of the output mode \hat{b} [Fig. 3(d)]. In the Supplemental Material [44], we extend the quantum-trajectory formalism beyond the truncated subspace considered here to accurately describe the photon subtraction also for long pulses with $\tau > \Gamma^{-1}$.

Efficient generation of non-Gaussian states—In the literature, the photon subtraction processes described by an annihilation operator \hat{a} is a highly non-Gaussian operation, which can be applied on a wide class of input states to distill states with a nonpositive Wigner function [18–20]. In linear optics, \hat{a} is implemented as the effect of a (rare) heralding process in which a single photon is detected in the signal reflected by a beam splitter. To suppress multiphoton subtraction events, one has to choose a relatively small reflectance, which inevitably reduces the success probability. In contrast, multiphoton subtraction is intrinsically suppressed by the two-level nonlinearity in the TLE-based subtraction discussed above. Our scheme thus holds promise to enable more efficient schemes for the heralded production of nonclassical states.

The TLE-based photon subtraction transforms a superposition state $\sum_n c_n |n\rangle$ into $\sum_n c_n f(n) |n-1\rangle$, conditioned on successful subtraction of a single photon in a given temporal mode [44]. When $n\Gamma\tau < 1$, the filtering function $f(n)$ approaches the solution of the quantum Rabi oscillations, and hence, the ideal one of a photon annihilation, i.e., $f(n) \approx \sin \sqrt{2\pi^{1/2}n\Gamma\tau} \sim \sqrt{n}$. To demonstrate the potential for generation of nonclassical states in this interaction regime, we consider generating a Schrödinger cat state $|\text{cat}\rangle \propto [|\alpha\rangle + (-1)^M |-\alpha\rangle]$ from a squeezed vacuum state via M successive photon subtractions [47], where $|\alpha\rangle$ denotes a coherent state with mean photon number $|\alpha|^2 = M$. The setup is illustrated in Fig. 4(a), where a quantum pulse gate (QPG) [48–50] is used to distill the state in the input temporal mode \hat{a} , while detection of photons in orthogonal temporal modes heralds a successful

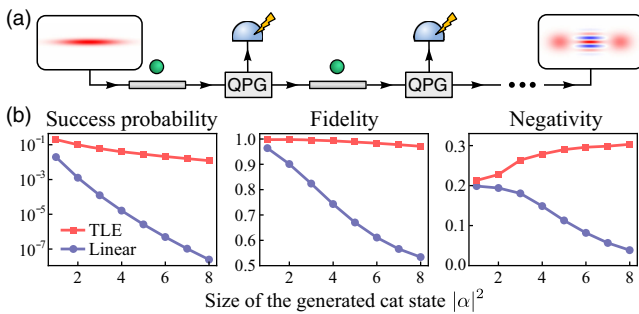


FIG. 4. (a) Generation of cat states from a squeezed vacuum state by successive single-photon subtractions. (b) Performance of the TLE scheme ($\Gamma\tau = 0.04$) and the linear scheme ($R = 0.01$) for a 10 dB initial squeezing. The output state is optimally unsqueezed to achieve the largest fidelity. The input and output blocks in (a) display the Wigner functions for the input state and the generated cat state ($|\alpha|^2 = 6$).

photon subtraction. The relation between the heralded state $\hat{\rho}_{\text{out}}$ and the input state $\hat{\rho}_{\text{in}}$ for each subtraction process is given by $\hat{\rho}_{\text{out}} = \hat{\rho}^a - \hat{U}_{\text{eff}}(\infty, 0)\hat{\rho}_{\text{in}}\hat{U}_{\text{eff}}^\dagger(\infty, 0)$, where $\hat{\rho}^a$ follows the master equation evolution [Eqs. (1) and (2)], while the second term describes the evolution of $\hat{\rho}_{\text{in}}$ conditioned on zero detector clicks [44].

We compare the typical performance of our scheme and the linear scheme in Fig. 4(b), where the parameters ($\Gamma\tau = 0.04$ and reflectance $R = 0.01$) are chosen after balancing the trade-off between efficiency and operation fidelity. As expected, the TLE-based subtractor has a significantly larger success probability as well as a better scaling with the number of operations. In addition, the fidelity and negativity of the generated state remain high in the TLE-based scheme, as multiphoton subtraction events are largely suppressed. The state fidelity can be further increased at the cost of a reduced success probability by merely choosing a smaller $\Gamma\tau$. Without further optimization, the performance of the TLE-based subtraction is comparable to an advanced, generalized subtraction scheme [47], which needs number-resolved photon detectors that are not required here.

Deterministic photon addition—The parity-time symmetry of the system allows us to apply a conjugate operation of the photon subtraction, i.e., deterministically adding a single photon in mode $\phi_b^T(t) = \phi_b^*(T-t)$ to mode $\phi_a^T(t) = \phi_a^*(T-t)$ carrying $n-1$ photons [see dashed arrows in Fig. 1(a)], where T should be sufficiently large to complete the pulses. The success probability $P_n^a = \rho_{n,n}^a$ of the single-photon addition is identical to the success probability $P_n^s = \rho_{n-1,n-1}^s$ of the single-photon subtraction due to a generalized reciprocity theorem [44]. This is verified by the numerical simulation shown in Fig. 5, where the success probability P_n^a and P_n^s at the optimal duration coincide and approach unity as n increases. Here, we identify a power-law scaling of the failure probability $1 - P_n^a \sim n^{-\beta}$ with $\beta \approx 1.23$. We note that the exponent $\beta > 1$ is formally due to the interaction with the auxiliary mode, without which we would expect $\beta = 1$ from the intuitive JC model.

The large success probability and its superior scaling property allows one to efficiently compose a large Fock

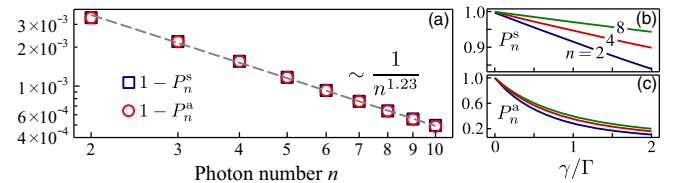


FIG. 5. (a) Scaling of the failure probability for optimal single-photon subtractions (blue squares) and additions (red squares). The dashed line denotes the power-law fitting to the data. (b) and (c) show the success probability of optimal single-photon subtractions and additions as a function of the imperfect coupling strength γ .

state from individual single photons. Specifically, by cascading the single-photon addition $|n-1\rangle \otimes |1\rangle \rightarrow |n\rangle \otimes |0\rangle$ from $n=2$ to $n=M$, one can create an M -photon Fock state with a success probability $P_M = \prod_{n=2}^M P_n^a$. The scaling factor $\beta > 1$ obtained in Fig. 5(a) implies that ideally an arbitrarily large Fock state can be generated with a finite success probability: for all M , $P_M > 96.7\%$, in stark contrast to exponentially decreasing success probabilities in a probabilistic scheme. The practical implementation of our scheme is illustrated in Fig. 1(b), where high-purity single photons in different pulse shapes are independently generated [51–54] and subsequently combined by a QPG, followed by the scattering on the TLE with an optimal interaction strength $\Gamma \propto 1/n$.

So far, the discussion is based on an ideal model where the TLE perfectly couples to the forward propagating mode. For an imperfect coupling, the scattering into the backward mode or free-space modes can be described by an additional decay rate γ . Figures 5(b) and 5(c) show the performance of the subtraction and addition with a finite γ . While both P_n^s and P_n^a decrease as γ/Γ increases, they are no longer identical. In particular, the subtraction process appears to be much more robust against imperfections than the addition. This is because P_n^s does not depend on details of the field modes orthogonal to the input one. As n increases further, P_n^s will approach unity due to suppressed multiphoton subtractions, while P_n^a will approach the branching ratio $\beta = \Gamma/(\gamma + \Gamma)$. In state-of-the-art waveguide QED setups, β can be made up to $\sim 99\%$ [55], which makes the implementation of the subtraction or addition scheme quite achievable.

Conclusion and outlook—In summary, we have examined the scattering of a unidirectional wave packet of light by a two-level emitter, and identified a near-perfect photon subtraction and addition to occur for pulses in the right temporal mode. We have offered intuitive and consistent descriptions of the process, explaining its crude features and offering very accurate accounts of its origin. The deterministic character of the demonstrated process enables efficient generation of large-size cat states and Fock states, offering indispensable resources for photonic quantum information processing [56,57]. The results and analysis apply also for microwave and acoustic waves scattering on, e.g., superconducting elements, and can be generalized to treat systems containing multiple waveguide channels [58]. Our effective analysis with an auxiliary mode provides a bridge between cavity and waveguide QED and causes optimism for further exploration of quantum nonlinear optics with traveling pulses.

Acknowledgments—We thank Anton L. Andersen, Šimon Bräuer, Ying Wang, and Anders S. Sørensen for helpful discussions. This work is supported by the Carlsberg Foundation through the “Semper Ardens” Research Project QCooL.

- [1] F. Flamini, N. Spagnolo, and F. Sciarrino, Photonic quantum information processing: A review, *Rep. Prog. Phys.* **82**, 016001 (2018).
- [2] S. Slussarenko and G. J. Pryde, Photonic quantum information processing: A concise review, *Appl. Phys. Rev.* **6**, 041303 (2019).
- [3] B. Brecht, D. V. Reddy, C. Silberhorn, and M. G. Raymer, Photon temporal modes: A complete framework for quantum information science, *Phys. Rev. X* **5**, 041017 (2015).
- [4] J. Wang, F. Sciarrino, A. Laing, and M. G. Thompson, Integrated photonic quantum technologies, *Nat. Photonics* **14**, 273 (2020).
- [5] H.-S. Zhong *et al.*, Quantum computational advantage using photons, *Science* **370**, 1460 (2020).
- [6] U. L. Andersen, T. Gehring, C. Marquardt, and G. Leuchs, 30 years of squeezed light generation, *Phys. Scr.* **91**, 053001 (2016).
- [7] S. D. Bartlett, B. C. Sanders, S. L. Braunstein, and K. Nemoto, Efficient classical simulation of continuous variable quantum information processes, *Phys. Rev. Lett.* **88**, 097904 (2002).
- [8] J. Eisert, S. Scheel, and M. B. Plenio, Distilling Gaussian states with Gaussian operations is impossible, *Phys. Rev. Lett.* **89**, 137903 (2002).
- [9] J. Fiurášek, Gaussian transformations and distillation of entangled Gaussian states, *Phys. Rev. Lett.* **89**, 137904 (2002).
- [10] G. Giedke and J. Ignacio Cirac, Characterization of Gaussian operations and distillation of Gaussian states, *Phys. Rev. A* **66**, 032316 (2002).
- [11] A. Mari and J. Eisert, Positive Wigner functions render classical simulation of quantum computation efficient, *Phys. Rev. Lett.* **109**, 230503 (2012).
- [12] A. Ourjoumtsev, F. Ferreyrol, R. Tualle-Brouri, and P. Grangier, Preparation of non-local superpositions of quasi-classical light states, *Nat. Phys.* **5**, 189 (2009).
- [13] H. Takahashi, J. S. Neergaard-Nielsen, M. Takeuchi, M. Takeoka, K. Hayasaka, A. Furusawa, and M. Sasaki, Entanglement distillation from Gaussian input states, *Nat. Photonics* **4**, 178 (2010).
- [14] D. Braun, P. Jian, O. Pinel, and N. Treps, Precision measurements with photon-subtracted or photon-added Gaussian states, *Phys. Rev. A* **90**, 013821 (2014).
- [15] Y.-S. Ra, C. Jacquard, A. Dufour, C. Fabre, and N. Treps, Tomography of a mode-tunable coherent single-photon subtractor, *Phys. Rev. X* **7**, 031012 (2017).
- [16] Y.-S. Ra, A. Dufour, M. Walschaers, C. Jacquard, T. Michel, C. Fabre, and N. Treps, Non-Gaussian quantum states of a multimode light field, *Nat. Phys.* **16**, 144 (2020).
- [17] A. Zavatta, S. Viciani, and M. Bellini, Quantum-to-classical transition with single-photon-added coherent states of light, *Science* **306**, 660 (2004).
- [18] A. Ourjoumtsev, R. Tualle-Brouri, J. Laurat, and P. Grangier, Generating optical Schrödinger kittens for quantum information processing, *Science* **312**, 83 (2006).
- [19] J. S. Neergaard-Nielsen, B. M. Nielsen, C. Hettich, K. Mølmer, and E. S. Polzik, Generation of a superposition of odd photon number states for quantum information networks, *Phys. Rev. Lett.* **97**, 083604 (2006).
- [20] A. Ourjoumtsev, A. Dantan, R. Tualle-Brouri, and P. Grangier, Increasing entanglement between Gaussian states

- by coherent photon subtraction, *Phys. Rev. Lett.* **98**, 030502 (2007).
- [21] J. Fiurášek, Engineering quantum operations on traveling light beams by multiple photon addition and subtraction, *Phys. Rev. A* **80**, 053822 (2009).
- [22] X. Zou, J. Shu, and G. Guo, Simple scheme for direct measurement of exponential phase moments of cavity fields by adiabatic passage, *Phys. Lett. A* **359**, 117 (2006).
- [23] L. C. G. Govia, E. J. Pritchett, S. T. Merkel, D. Pineau, and F. K. Wilhelm, Theory of Josephson photomultipliers: Optimal working conditions and back action, *Phys. Rev. A* **86**, 032311 (2012).
- [24] D. K. L. Oi, V. Potoček, and J. Jeffers, Nondemolition measurement of the vacuum state or its complement, *Phys. Rev. Lett.* **110**, 210504 (2013).
- [25] J. Gea-Banacloche and W. Wilson, Photon subtraction and addition by a three-level atom in an optical cavity, *Phys. Rev. A* **88**, 033832 (2013).
- [26] J. Du, W. Li, and M. Bajcsy, Deterministic single-photon subtraction based on a coupled single quantum dot-cavity system, *Opt. Express* **28**, 6835 (2020).
- [27] S. Rosenblum, O. Bechler, I. Shomroni, Y. Lovsky, G. Guendelman, and B. Dayan, Extraction of a single photon from an optical pulse, *Nat. Photonics* **10**, 19 (2016).
- [28] C. Tresp, C. Zimmer, I. Mirgorodskiy, H. Gorniaczyk, A. Paris-Mandoki, and S. Hofferberth, Single-photon absorber based on strongly interacting Rydberg atoms, *Phys. Rev. Lett.* **117**, 223001 (2016).
- [29] N. Stiesdal, H. Busche, K. Kleinbeck, J. Kumlin, M. G. Hansen, H. P. Büchler, and S. Hofferberth, Controlled multi-photon subtraction with cascaded Rydberg superatoms as single-photon absorbers, *Nat. Commun.* **12**, 4328 (2021).
- [30] C. R. Murray, I. Mirgorodskiy, C. Tresp, C. Braun, A. Paris-Mandoki, A. V. Gorshkov, S. Hofferberth, and T. Pohl, Photon subtraction by many-body decoherence, *Phys. Rev. Lett.* **120**, 113601 (2018).
- [31] A. V. Gorshkov, R. Nath, and T. Pohl, Dissipative many-body quantum optics in Rydberg media, *Phys. Rev. Lett.* **110**, 153601 (2013).
- [32] F. Yang, Y.-C. Liu, and L. You, Atom-photon spin-exchange collisions mediated by Rydberg dressing, *Phys. Rev. Lett.* **125**, 143601 (2020).
- [33] D. Roy, C. M. Wilson, and O. Firstenberg, Colloquium: Strongly interacting photons in one-dimensional continuum, *Rev. Mod. Phys.* **89**, 021001 (2017).
- [34] D. E. Chang, J. S. Douglas, A. González-Tudela, C.-L. Hung, and H. J. Kimble, Colloquium: Quantum matter built from nanoscopic lattices of atoms and photons, *Rev. Mod. Phys.* **90**, 031002 (2018).
- [35] A. S. Sheremet, M. I. Petrov, I. V. Iorsh, A. V. Poshakinskiy, and A. N. Poddubny, Waveguide quantum electrodynamics: Collective radiance and photon-photon correlations, *Rev. Mod. Phys.* **95**, 015002 (2023).
- [36] A. H. Kiilerich and K. Mølmer, Input-output theory with quantum pulses, *Phys. Rev. Lett.* **123**, 123604 (2019).
- [37] A. H. Kiilerich and K. Mølmer, Quantum interactions with pulses of radiation, *Phys. Rev. A* **102**, 023717 (2020).
- [38] V. R. Christiansen, A. H. Kiilerich, and K. Mølmer, Interactions of quantum systems with pulses of quantized radiation: From a cascaded master equation to a traveling mode perspective, *Phys. Rev. A* **107**, 013706 (2023).
- [39] M. M. Lund, F. Yang, and K. Mølmer, Perfect splitting of a two-photon pulse, *Phys. Rev. A* **107**, 023715 (2023).
- [40] T. Caneva, M. T. Manzoni, T. Shi, J. S. Douglas, J. I. Cirac, and D. E. Chang, Quantum dynamics of propagating photons with strong interactions: A generalized input–output formalism, *New J. Phys.* **17**, 113001 (2015).
- [41] X. H. H. Zhang and H. U. Baranger, Quantum interference and complex photon statistics in waveguide QED, *Phys. Rev. A* **97**, 023813 (2018).
- [42] O. A. Iversen and T. Pohl, Self-ordering of individual photons in waveguide QED and Rydberg-atom arrays, *Phys. Rev. Res.* **4**, 023002 (2022).
- [43] W.-L. Li, G. Zhang, and R.-B. Wu, On the control of flying qubits, *Automatica* **143**, 110338 (2022).
- [44] See Supplemental Material at <http://link.aps.org/supplemental/10.1103/PhysRevLett.133.103601> for derivations of the effective master equation, a general quantum-trajectory treatment, analysis of the two-photon scattering, proof of the reciprocity theorem, details about the cat state generation, and experimental considerations, which includes Refs. [45,46].
- [45] A. Blais, A. L. Grimsmo, S. M. Girvin, and A. Wallraff, Circuit quantum electrodynamics, *Rev. Mod. Phys.* **93**, 025005 (2021).
- [46] J. Vaneecloo, S. Garcia, and A. Ourjoumtsev, Intracavity Rydberg superatom for optical quantum engineering: Coherent control, single-shot detection, and optical π phase shift, *Phys. Rev. X* **12**, 021034 (2022).
- [47] K. Takase, J. I. Yoshikawa, W. Asavanant, M. Endo, and A. Furusawa, Generation of optical Schrödinger cat states by generalized photon subtraction, *Phys. Rev. A* **103**, 013710 (2021).
- [48] A. Eckstein, B. Brecht, and C. Silberhorn, A quantum pulse gate based on spectrally engineered sum frequency generation, *Opt. Express* **19**, 13770 (2011).
- [49] B. Brecht, A. Eckstein, R. Ricken, V. Quiring, H. Suche, L. Sansoni, and C. Silberhorn, Demonstration of coherent time-frequency Schmidt mode selection using dispersion-engineered frequency conversion, *Phys. Rev. A* **90**, 030302 (R) (2014).
- [50] L. Serino, J. Gil-Lopez, M. Stefszky, R. Ricken, C. Eigner, B. Brecht, and C. Silberhorn, Realization of a multi-output quantum pulse gate for decoding high-dimensional temporal modes of single-photon states, *PRX Quantum* **4**, 020306 (2023).
- [51] I. Söllner, S. Mahmoodian, S. L. Hansen, L. Midolo, A. Javadi, G. Kiršanské, T. Pregolato, H. El-Ella, E. H. Lee, J. D. Song, S. Stobbe, and P. Lodahl, Deterministic photon–emitter coupling in chiral photonic circuits, *Nat. Nanotechnol.* **10**, 775 (2015).
- [52] C. J. Axline, L. D. Burkhardt, W. Pfaff, M. Zhang, K. Chou, P. Campagne-Ibarcq, P. Reinhold, L. Frunzio, S. M. Girvin, L. Jiang, M. H. Devoret, and R. J. Schoelkopf, On-demand quantum state transfer and entanglement between remote microwave cavity memories, *Nat. Phys.* **14**, 705 (2018).
- [53] W. Pfaff, C. J. Axline, L. D. Burkhardt, U. Vool, P. Reinhold, L. Frunzio, L. Jiang, M. H. Devoret, and R. J. Schoelkopf,

- Controlled release of multiphoton quantum states from a microwave cavity memory, *Nat. Phys.* **13**, 882 (2017).
- [54] J. Yang, A. M. Eriksson, M. A. Aamir, I. Strandberg, C. Castillo-Moreno, D. P. Lozano, P. Persson, and S. Gasparinetti, Deterministic generation of shaped single microwave photons using a parametrically driven coupler, *Phys. Rev. Appl.* **20**, 054018 (2023).
- [55] L. Scarpelli, B. Lang, F. Masia, D. M. Beggs, E. A. Muljarov, A. B. Young, R. Oulton, M. Kamp, S. Höfling, C. Schneider, and W. Langbein, 99% beta factor and directional coupling of quantum dots to fast light in photonic crystal waveguides determined by spectral imaging, *Phys. Rev. B* **100**, 035311 (2019).
- [56] J. Hastrup and U. L. Andersen, All-optical cat-code quantum error correction, *Phys. Rev. Res.* **4**, 043065 (2022).
- [57] A. Ourjoumtsev, H. Jeong, R. Tualle-Brouri, and P. Grangier, Generation of optical ‘Schrödinger cats’ from photon number states, *Nature (London)* **448**, 784 (2007).
- [58] J. Lindkvist and G. Johansson, Scattering of coherent pulses on a two-level system–single-photon generation, *New J. Phys.* **16**, 055018 (2014).